JOURNAL OF PROPULSION AND POWER
Vol. 18, No. 5, September–October 2002

High-Speed Centrifugal Compressor Surge Initiation Characterization

William C. Oakes* and Patrick B. Lawless†
Purdue University, West Lafayette, Indiana 47907
John R. Fagan‡
Light Engineering, Indianapolis, Indiana 46268
and
Sanford Fleeter§
Purdue University, West Lafayette, Indiana 47907

An experimental study is performed to characterize the behavior of a high-speed centrifugal compressor as it approaches instability. To achieve this, data at the inlet and exit of the centrifugal compressor are analyzed. Three inducer bleed conditions are examined. Data analysis indicates that the disturbance was a 9-lobed stall pattern occurring in or near the diffuser and suggests that the phenomena is different than that typically referred to as impeller stall. The component pressure characteristics show a reduction in diffuser performance corresponding to the rise in the spatial mode magnitude, with minimal effect on the impeller. It is suggested that the rotating stall condition that was observed in this compressor may play a similar role to that observed when rotating stall initiates surge in multistage axial compressor.

Nomenclature

A = inlet area
m = mass flow rate
P = static pressure
U = wheel speed based on mean inlet radius
ρ = air density at impeller inlet
ϕ = flow coefficient, $m/\rho U A$
Ψ = pressure coefficient, $P - P_0/\rho U^2$

Subscripts

0 = impeller inlet
1 = impeller exit
2 = diffuser inlet
3 = plenum

Introduction

ON the aerodynamic performance map of a compression system, the operating range is bounded by the surge and choke lines. The barrier posed by the surge line is of particular interest due to its proximity to the maximum efficiency points of the compressor. The surge line separates the regions of stable and unstable compressor operation. Modern compressors allow for a safety margin, known as the surge margin, which places the operating point in a region that guarantees stable operation. If this margin is not maintained, small changes in compressor operation can result in compression system instability, generally characterized as either surge or rotating stall. Surge is a circumferentially uniform global flow oscillation through the compression system. In contrast, rotating stall is a circumferentially nonuniform flow disturbance that propagates around the compressor annulus at a fraction of wheel speed.

The disadvantages of operating a compressor in a stall or surge condition are twofold. First, the compression system performance falls off dramatically. For flight application, such a loss of performance can result in a catastrophic loss of thrust. Second, as discussed by Haupt et al.,[1] and Jin et al.,[2,3] rotating stall and surge represent dangerous unsteady aerodynamic excitations to impeller and diffuser vanes. These serious consequences, together with the highest compressor efficiency being near the surge line, have made increasing the stable operating range of compressors an area of vigorous research activity. Increasing the stable operating range of a compressor requires understanding the instability itself and the phenomena preceding the stall or surge. To this end, investigations of rotating stall in axial compressors have included those of Day,[4] McDougall et al.,[5] and Garnier et al.[6]. Analogous studies have been performed on centrifugal compressors by Lawless and Fleeter.[7]

Compressor instability studies have primarily been performed on low-speed research compressors, where compressibility effects are not important. High-speed compressor instability inception experiments have largely focused on axial compressors, where rotating stall is a significant contributor to both fully developed stall and surge.[8,9]

The understanding of disturbances at the initiation of surge is critical to the eventual control of these instabilities. Ffowcs Williams and Graham[10] were concerned with the suppression of developed surge. Ffowcs Williams et al.[11] focused on the suppression of developed nonaxisymmetric disturbances and noted but did not investigate the occurrence of a periodic disturbance occurring before surge. However, in contrast to high-speed axial compressors, there is a dearth of high-speed centrifugal compressor instability initiation information.

To begin to provide the needed high-speed centrifugal compressor instability initiation information, this paper is directed at characterizing the surge initiation process of a high-speed centrifugal compressor typical of those employed in aero propulsion applications. To this end, high-response dynamic pressure transducers are installed in the Purdue High-Speed Centrifugal Research Compressor inlet and exit plenum. Data from these transducers are acquired as the compressor is slowly throttled into surge. Both time–frequency spectral- and spatial-domain analysis techniques are employed to characterize the instability signature. Quasi-steady, static pressure measurements are also taken at the inlet and exit of the impeller

Received 27 July 2001; revision received 8 March 2002; accepted for publication 25 March 2002.

*Assistant Professor, Freshman Engineering. Member AIAA.
†Associate Professor, School of Mechanical Engineering. Member AIAA.
‡Vice President, Engineering. Member AIAA.
§McAllister Distinguished Professor, School of Mechanical Engineering. Fellow AIAA.

and diffuser that allow the component performance to be measured before and during surge.

Facility and Instrumentation

Purdue High-Speed Centrifugal Research Compressor

The primary components of the Purdue High-Speed Centrifugal Research Compressor Facility are an Allison 250-C30G engine (C30), a slave gearbox (SGB), and a centrifugal research compressor (RC) (Fig. 1). The C30 is a turboshaft engine producing 550 shaft hp (415 kW). The drive engine is connected to the SGB by a low-speed shaft. The SGB is a highly modified Allison gearbox from a C30. A high-speed shaft connects the SGB to the RC. These components are individually mounted a test base in the center of the test stand. The peripheral support equipment includes an oil system, a fuel system, an air handling system, an electrical and controls system, a fire suppression system and the research compressor instrumentation.

The compressor, shown schematically in Fig. 2, was designed by the Allison Engine Company and consists of a titanium impeller, a radial-vaned diffuser, a discharge plenum, and a bearing housing to support the compressor shaft. The centrifugal impeller has a nominal operating speed of 48,450 rpm, a maximum pressure ratio of 5.4, and a maximum mass flow rate of 5.5 lbm/s (2.5 kg/s). There are 36 inducer bleed slots spaced circumferentially around the compressor shroud 0.5 in. (1.3 cm) from the impeller leading edge. The design and performance parameters of the RC are presented in Table 1.

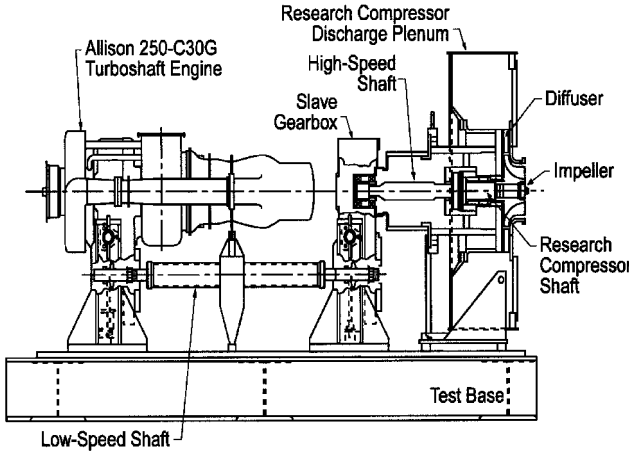

Fig. 1 Main components of the Purdue High-Speed Research Compressor facility.

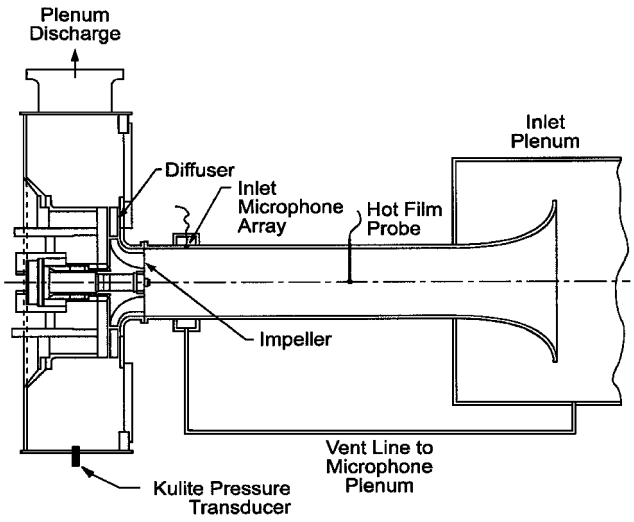

Fig. 2 Compressor instrumentation.

Table 1 RC parameters

Parameter	Value
Impeller	
Tip diameter, in. (cm)	8.5 (21.6)
Inlet diameter, in. (cm)	5.6 (14.2)
Number of blades	15 with splitters
Design speed, rpm	48,450
Maximum pressure ratio	5.4
Maximum flow rate, lb/s (kg/s)	5.5
Diffuser	
Inlet diameter, in. (cm)	9.4 (23.9)
Exit diameter, in. (cm)	13.6 (34.5)
Number of vanes	22
Axial passage width, in. (cm)	0.55 (1.4)
Plenum	
Outside diameter, in. (cm)	33 (83.8)
Axial length, in. (cm)	10 (25.4)

Before the air enters the impeller, the air is passed through a series of screens and honeycombs to reduce the compressor inlet pressure. This both decreases the power required from the driving engine and also reduces the mechanical strain during the surge and stall experiments. After the inlet air passes through the screens and honeycomb, it enters a plenum where additional screens and honeycomb form a modified Sprenkle to reduce flow disturbances. At the end of the plenum, a contraction brings the air to the impeller inlet. Inlet surveys have shown that the impeller inlet flow is uniform.[12]

After the air passes through the impeller and the vaned diffuser, it discharges into the collection plenum and then exhausts out one side. The compressor is throttled by a butterfly valve driven by a gear motor in the exhaust pipe. Downstream of the valve and flow straighteners is a vortex flow meter to measure the compressor flow rate.

Instrumentation

An array of eight equally spaced PCB103A miniature microphones is mounted in the end wall of the impeller inlet, 3.25 in. (8.26 cm) upstream of the impeller (Fig. 2). To eliminate blade and splitter pass frequencies, a passive third-order RC antialiasing filter with a cutoff frequency of 2200 Hz is used. The microphones were dynamically calibrated to account for nonlinearities of the filters. Because the inlet of the compressor is at subatmospheric pressure, a plenum chamber is mounted over the microphone array. This chamber is vented to the inlet plenum to equalize the steady pressure across the microphones.

A single Kulite® XTE-190 dynamic pressure transducer is mounted in the discharge plenum opposite from the plenum discharge port. An Omega PX212 pressure transducer is mounted in the endwall of the inlet plenum to measure inlet total pressure. The same model transducer is also used to measure the impeller exit and diffuser inlet pressure. These locations are measured through static pressure taps in the shroud that eliminates the need for high-temperature transducers but provides sufficient frequency response to characterize the compressor performance before and during surge events.

Experimental Technique

For this investigation, three inducer bleed flow conditions are examined. First, the inducer bleed slots in the shroud are closed. In the second configuration, there is partial bleed. The third condition involves completely open bleed slots. All three conditions are examined at a constant impeller corrected speed of 90% design speed.

Compressor Stalling Behavior

The inlet array of microphones and the plenum dynamic pressure transducer are employed to characterize the stalling behavior of the compressor. After the compressor achieves a steady operating point with the throttle valve open, the valve is closed at a constant rate.

This moves the compressor toward instability. Data acquisition is initiated at the beginning of the throttle movement and continues until the trigger level of a selected inlet microphone is reached and the compressor has destabilized. The dynamic pressure transducer and microphone signals are sampled at a rate of 8000 Hz using three National Instruments EISA-A2000 analog-to-digital conversion boards installed in a Micron P133 Powerserver SMP computer, which allows 12 channels of data to be recorded simultaneously. Once the trigger level is reached, 16,000 samples are stored with half the samples before the trigger. Continuous throttle movement occurs during the entire data acquisition sequence.

Compressor Pressure Characteristic

The quasi-steady performance of the compressor is characterized by measuring the impeller inlet total pressure P_0, impeller exit static pressure P_1, diffuser inlet static pressure P_2, and plenum pressure P_3, as well as the mass flow. The mass flow is measured using a hot-film sensor mounted in the impeller inlet section and calibrated against the vortex flow meter. After the compressor achieves a steady operating point with the throttle valve open, the valve is closed at a constant rate. Data acquisition is initiated when the throttle is closed 30% and continues at a sampling rate of 8000 Hz for 6 s. This provides a window of data that includes the presurge operation as well as several surge cycles. The data are then time averaged over 0.017 s.

Data Analysis

Fourier analysis of signals from an array of circumferentially distributed simultaneously sampled microphones has proven effective in identifying spatially coherent phenomena such as rotating stall.[7] In such a technique, the Fourier transform is performed in the spatial domain on a simultaneous signal from each microphone in an array. Before the Fourier transform, the inlet microphone signals are numerically filtered between 1400 and 1500 Hz using a third-order Butterworth bandpass filter. The resultant harmonics correspond to wave numbers or modes propagating around the compressor annulus.

Another technique employed is a joint time–frequency analysis that is performed on a single inlet microphone and the plenum pressure transducer to identify frequency bands where instability is encountered. The joint time–frequency analysis consists of performing a Fourier transform on a fraction of the data, or window, and then repeating the process by advancing the window by a short time. The resultant spectra then form a transient plot of the instability frequencies. The data are scaled in the frequency domain to account for the nonlinearities introduced by the antialiasing filters.

A second spatial Fourier analysis technique is also employed to resolve aliased modes. The noted spatial analysis produces an aliased mode-folding diagram, as shown in Table 2. Further resolution of aliased modes is accomplished by first taking a Fourier transform in time of a window of data for each microphone in the array and advancing the window by a short time, similar to the joint–time frequency analysis. The output of the Fourier transforms from each microphone corresponding to the frequency identified by the joint time–frequency analysis is then processed using a spatial Fourier transform. Because the result of the temporal transform contains phase as well as magnitude information, the direction of modes 1, 2, and 3 can be determined, thereby eliminating potential aliased modes noted in Table 2.

Table 2 Nyquist folding diagram for eight microphones

Parameters	Spatial mode				
Aliased modes (Nyquist = 4)				21	20
	16	17	18	19	20
	16	15	14	13	12
	8	9	10	11	12
	8	7	6	5	4
Modes represented in Fourier transform	0	1	2	3	4

Results

Joint Time–Frequency Analysis

Open Inducer Bleed

Figure 3 shows the pressure traces from the plenum dynamic pressure transducer and one inlet microphone as the throttle is slowly closed for the open inducer bleed case. Time is scaled by rotor pass period and is, therefore, shown in impeller revolutions. The first surge cycle begins at $t = 600$ rotor revolutions and is preceded by a period of approximately 200 revolutions, where a high-frequency disturbance is apparent in the plenum signal trace. This disturbance manifests itself as two brief eruptions at 350 and 400 revolutions, followed by a sustained presence from $t = 450$ revolutions until the pressure delivery of the compressor falls as the first surge cycle initiates.

Figure 4 shows the joint time–frequency analysis of this plenum pressure transducer signal. The disturbance before surge onset consists of a discrete frequency, centered around 1450 Hz (point A). This frequency is consistent with a multiple-cell rotating stall condition. The frequency content of this signal is constant until the first surge cycle, where the disturbance vanishes. It reappears at the start of later surge cycles, as shown by point B. This behavior appears to be similar to axial flow compressor

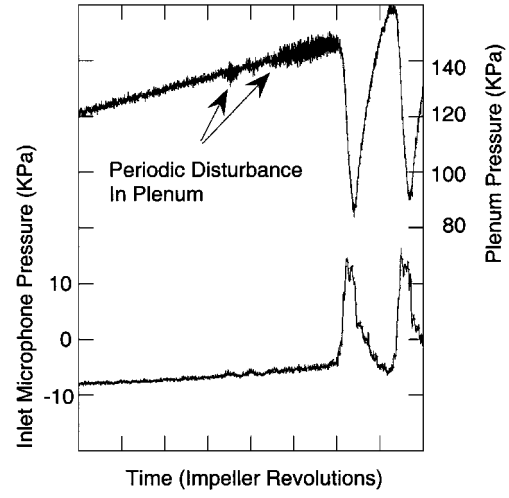

Fig. 3 Comparison of inlet microphone and scroll pressure transducer signals.

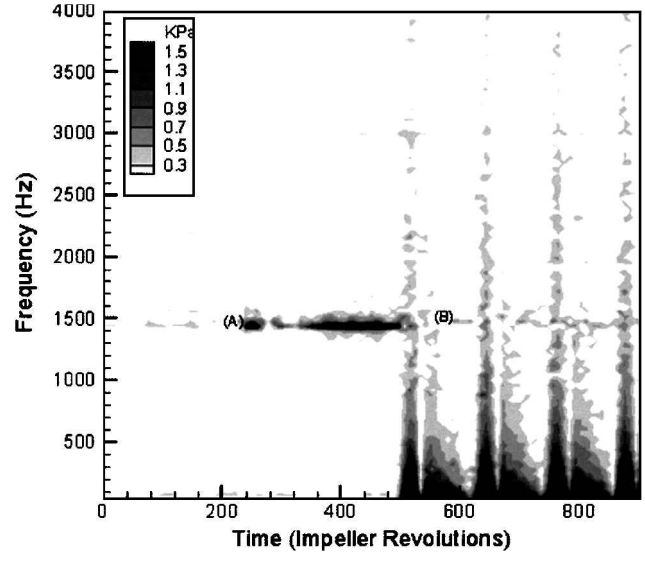

Fig. 4 Joint time–frequency analysis of the scroll pressure transducer, open bleed.

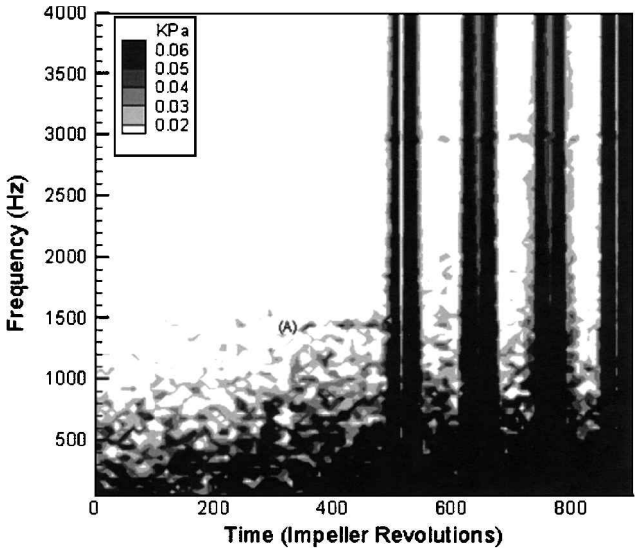

Fig. 5 Joint time–frequency analysis of one inlet microphone, open bleed.

surge where rotating stall is often observed initiating the surge cycle.[8,9]

Figure 5 shows the joint time–frequency analysis for one of the inlet microphones. The amplitude of the disturbance is much lower in the inlet, and therefore, the signal to noise ratio is significantly decreased. On this scale, the aliased blade pass frequency appears, shown by point B. However at point A, a rise in signal magnitude at 1450 Hz occurs. This signal corresponds to the disturbance indicated by the plenum pressure transducer and continues until the first surge cycle.

Figures 4 and 5 show that, whereas the discrete disturbance is detected at both the plenum and the inlet, it is two orders of magnitude larger in the plenum. This suggests that the disturbance is located near the diffuser section of the compressor, and the signal is attenuated as it propagates to the inlet section. Frigne and Van Den Braembussche reported a similar behavior for a diffuser rotating stall condition in a 2:1 pressure ratio centrifugal compressor with a vaneless diffuser, where the stall condition was significantly attenuated at the impeller inlet.[13] However, little additional information is available on the propagation or behavior of rotating stall in machines that demonstrate high-speed/transonic flow in the diffuser section.

The size of the data windowing for the preceding Fourier analysis was 200 samples, resulting in a frequency resolution of 40 Hz. To improve this resolution, a 2000 sample window (186 impeller revolutions) was analyzed from a section of the signal trace where the disturbance was present. The results from this transform are presented in Fig. 6, where the peak magnitude is indicated at $1452 + 4$ Hz.

Partial Inducer Bleed

When the case with partial inducer bleed is examined using the joint time–frequency analysis, a similar surge initiation behavior is found. The amplitude of the disturbance is 30% less than for the open inducer bleed. The disturbance also rises earlier during the throttling of the compressor and persists for a longer period (400 vs 200 revolutions). The amplitude of the disturbance is, however, less stable, showing areas where it decays and then grows again as it approaches the first surge cycle.

Closed Inducer Bleed

An even more marked difference in the surge initiation behavior occurs when the inducer bleed slots are closed, as seen in Fig. 7. The disturbance is again observed, but rises in magnitude at point A only 25 impeller revolutions before the first surge cycle. The amplitude of the signal at point A is similar to the amplitude with partial

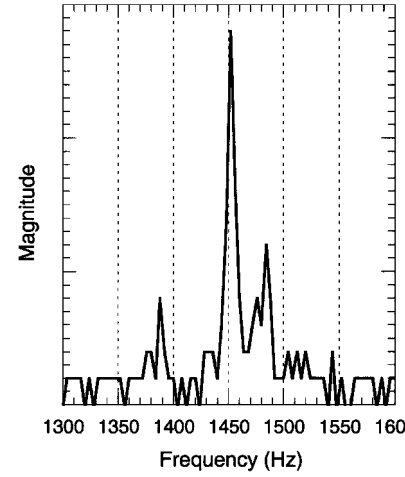

Fig. 6 Fourier transform of scroll pressure transducer during period of increased amplitude.

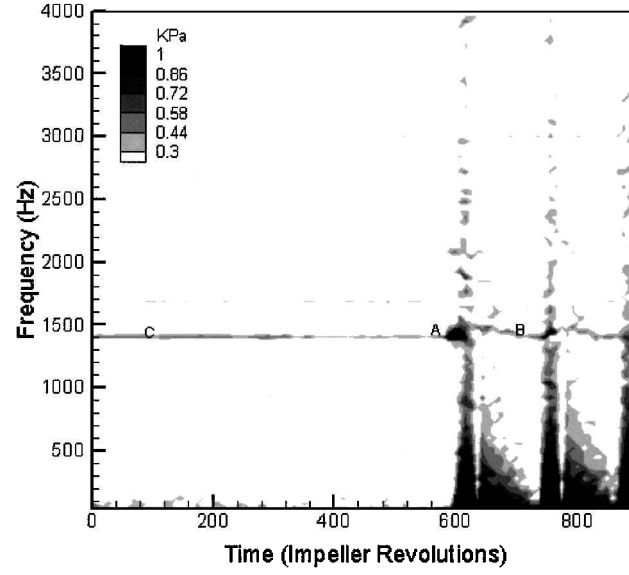

Fig. 7 Joint time–frequency analysis of the scroll pressure transducer, closed bleed.

bleed flow. At point B, the disturbance is again observed between subsequent surge cycles. A lower level signal is seen during the entire throttle near the frequency of the larger magnitude periodic disturbance, as shown by point C. This level is 25% of the magnitude of the disturbance at point A and occurs in a frequency range of 1420–1440 Hz. This signal is of unknown origin and does not correspond to any expected disturbance or aliased disturbance in the compressor.

Spatial-Domain Analysis

The results from the spatial Fourier analysis of the inlet microphones are shown in Fig. 8 for the first, second, and third spatial modes and the plenum pressure transducer for the case of open inducer bleed. At $t = 350$ and 400 revolutions, the first mode magnitude increases and then decays. The mode magnitude increases again at $t = 450$ and remains until $t = 600$ revolutions when the first surge cycle begins. This corresponds to the bursts seen in the plenum transducer signal. The second mode magnitude is also presented and shows increases in magnitude also at $t = 350$, 400, and 450. The increase in magnitude is less than for the first mode.

Resolution of Aliased Modes

The spatial-domain analysis clearly shows a spatial coherence demonstrated by the rise in the first and second mode magnitudes and

Table 3 Potential diffuser modes and rotational speed

Mode	% Impeller speed
1	195
7	28
9	22
15	13
17	11

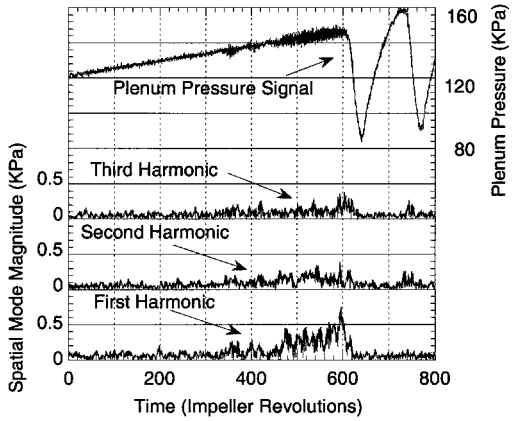

Fig. 8 Spatial mode magnitudes and scroll pressure transducer signal, open bleed.

is consistent with a nonsinusoidal rotating stall waveform. However, because impeller rotational frequency is 743 Hz, the frequency of the disturbance precludes the possibility that the information contained in the first mode is a result of a single-cell stall condition. Thus, the information obtained from the spatial Fourier transform must actually be a spatially aliased disturbance of higher cell count. Table 2 shows a Nyquist folding diagram for the inlet array of eight microphones, which indicates where aliased information will appear in an undersampled data set. Waveforms of modes 7, 9, 15, 17, etc., will fold into a first mode. Table 3 shows the modes and their rotational speed as a percentage of rotor speed. Modes 7, 9, 15, and 17 are all within reasonable speed ranges expected for a multiple-lobed rotating stall pattern.

The range of possible cell counts can be further reduced by analysis of a portion of the signal where the stall condition can be taken as fully developed and of invariant cell number and frequency. This is achieved by performing a temporal Fourier transform on the signal from each microphone in the spatial array and then performing a spatial Fourier transform on the complex coefficients determined by the temporal transform. The temporal transform thus provides the phase relationship between the microphone signals and, thereby, the direction of the wave.

Figure 9 shows the results of this analysis for the case of open bleed. Clearly, the $+1$ mode is the dominant mode. Aliased modes can be $+1, +8$ (the number of microphones in the array). The possible modes are then as follows: $\ldots, -15, -7, +1, +9, +17, \ldots$, As already noted, the $+1$ mode can be eliminated. Also, if the behavior of the disturbance is consistent with a system instability such as rotating stall, the pattern will propagate in the direction of the impeller (the positive modes). Therefore, the negative modes can be eliminated. Because the diffuser has 22 vanes, it is unlikely that the stall pattern would be a mode higher than the number of vanes. Therefore, the aliased information contained in the first mode results is likely due to a disturbance of 9 or 17 cells, with the 9-cell condition more consistent with cell counts observed in previous studies.

Table 2 shows that an aliased second harmonic of a nine-cell pattern would alias into the second mode magnitude bin. The relative magnitude with respect to the first mode is unexpectedly high when it is considered that the decay rate of the wave is proportional to the wave number. The attenuation seen from the aliased first-mode magnitude should lead to a further attenuation with a higher wave

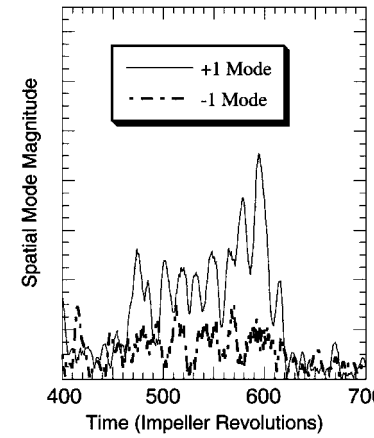

Fig. 9 Positive and negative first mode magnitudes, open bleed.

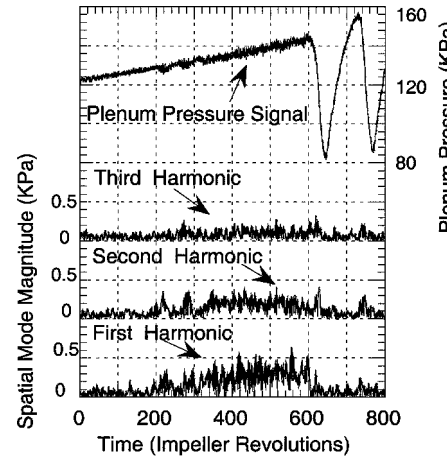

Fig. 10 Spatial mode magnitudes and scroll pressure transducer signal, partial bleed.

number from the second, third, etc., harmonics. The higher magnitudes of the harmonics may be the result of sympathetic events occurring near the inlet of the compressor. However, the poor signal-to-noise ratio makes accurate analysis of the modal information of this reduced magnitude difficult, and therefore, no significant conclusions can be drawn from this behavior.

Although the data contained in the spatial transform results are clearly aliased, they still provide useful information on the nature of the stall waveform as the frequency of the disturbance precludes that aliased information is distorted by actual (nonaliased) Fourier content in the first mode. The second, and higher, harmonics are not precluded from being distorted by actual Fourier content, although it is unlikely that multiple independent stall patterns would propagate at the same frequency.

Partial Inducer Bleed

Figure 10 shows the spatial modes and plenum signal for the case with partial inducer bleed. Again, there are bursts in the first-mode magnitude corresponding to the increase in amplitude of the plenum signal between $t = 200$ and 300 revolutions. A similar rise in the second-mode magnitude occurs in this region, indicative either of a nonsinusoidal waveform at the inlet or more complex inlet phenomena. As before, all of the content of these signal is believed to be the result of an aliased higher-order stall mode. It is only after $t = 400$ revolutions that the first-mode magnitude rises clearly above the other mode magnitudes.

Closed Inducer Bleed

Figure 11 shows the conditions for the case of inducer bleed closed. The plenum pressure shows the first surge cycle now occurs at a lower pressure ratio than the other two cases. The spatial-mode

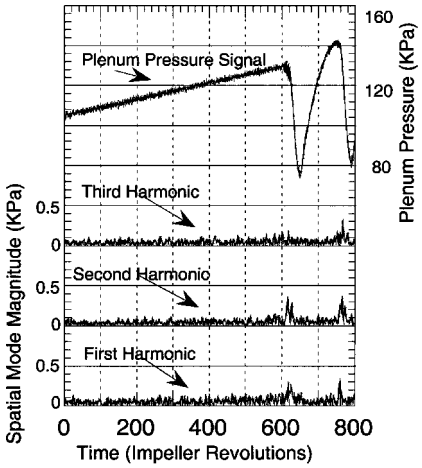

Fig. 11 Spatial mode magnitudes and scroll pressure transducer signal, closed bleed.

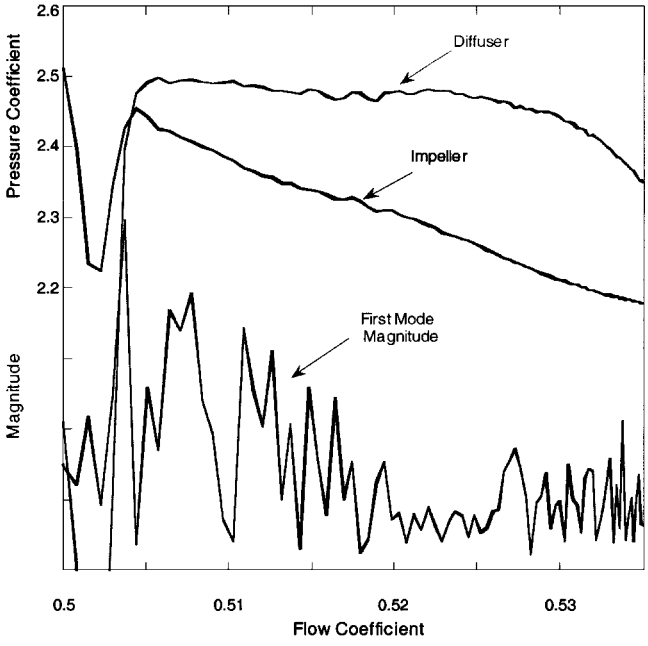

Fig. 12 Diffuser and impeller performance prior to surge.

magnitudes again show a rise in the first- (aliased nine-mode) and second-mode (second harmonic of the aliased nine-mode) magnitudes. Reflecting the results of the joint time-frequency analysis, the rise in mode magnitude occurs only 25 revolutions before the first surge cycle. Again, as with the initial eruptions in the earlier case, the short bursts of activity of the disturbance is characterized with a strong second harmonic content. In this case, the disturbance can also be detected in the third harmonic.

In all three cases, increases in mode magnitudes occur at the start of the second surge cycle, also consistent with the joint time–frequency analysis of Figs. 4 and 7. There is not, however, a consistent mode magnitude that dominates these bursts. In fact, in the case of the open bleed, little first-mode activity is detected in spite of the presence of a second mode. Again, this points to the possibility of a complex behavior of a sympathetic inlet disturbance or perhaps a transient cell count playing a role during the first stages of the development of the rotating stall phenomena.

Compressor Pressure Characteristic

The pressure characteristic is measured as the compressor is throttled into surge for the case of open bleed. This case was chosen because the disturbance magnitude is the largest of the three cases. Figure 12 shows the impeller performance Ψ_1 and the diffuser performance $\Psi_3-\Psi_2$ as the compressor is throttled, with a trace of the first-mode magnitude. At $\phi = 0.52$, the spatial-mode magnitude begins to increase, and the slope of the diffuser performance is reduced significantly. The impeller performance is not significantly affected by the rise in the spatial-mode magnitude. The reduction in diffuser pressure recovery indicates that the propagating disturbance is located in the diffuser section of the compressor, rather than the impeller. The diffuser performance will result in a change in the slope of the overall characteristic and, therefore, affect the stability of the compressor.[14]

Summary

The goal of this investigation was to characterize the surge initiation process in a high-speed centrifugal compressor typical of those employed in aeropropulsion applications. For this purpose, high-response dynamic pressure transducers were installed in the Purdue High Speed Centrifugal Research Compressor inlet and exit plenum. Data from these transducers were acquired as the compressor was slowly throttled into surge. Both time–frequency spectral- and spatial-domain analysis techniques were employed to characterize the instability signature. Quasi-steady, static pressure measurements were also taken at the inlet and exit of the impeller and diffuser that allowed the component performance to be measured before and during surge.

The results demonstrated that before the onset of surge, an apparent rotating stall condition erupted in the compressor. Analysis of the data indicated that the disturbance was likely a 9-lobed stall pattern. The signal is two orders of magnitude stronger in the exit plenum than in the inlet. This indicates that the rotating stall was most likely occurring in or near the diffuser and suggests that the phenomena is different than that typically referred to as impeller stall. The component pressure characteristics confirmed this by showing a reduction in diffuser performance as the first-spatial-mode magnitude rises. The significant attenuation of the signal from the diffuser rotating stall suggests that the stall may not be related to a system resonance and, perhaps, is a phenomenon isolated to the diffuser itself. However, little information is available on the propagation or behavior of rotating stall in machines that demonstrate high-speed/transonic flow in the diffuser section.

Although the inducer bleed flow was shown to have a significant effect on the surge point, the surge initiation behavior of the compressor was similar in all three conditions. It is suggested that the rotating stall condition that was observed in this compressor and the resulting reduction in diffuser performance may play a similar role to that observed when rotating stall initiates surge in multistage axial compressor.

Acknowledgments

This research sponsored in part by the Army Research Office. This support is most gratefully acknowledged. The work of Ronnie D. McGuire in support of this research is also gratefully acknowledged.

References

[1]Haupt, U., Abdel-Hamid, A. N., Kaemmer, N., and Rautenber, M., "Excitation of Blade Vibration by Flow Instability in Centrifugal Compressors," American Society of Mechanical Engineers, ASME Paper 86-GT-283, 1986.

[2]Jin, D., Haupt, U., Hasenmann, H., and Rautenberg, M., "Excitation of Blade Vibration Due to Surge of Centrifugal Compressors," American Society of Mechanical Engineers, ASME Paper 92-GT-149, 1992.

[3]Jin, D., Haupt, U., Hasenmann, H., and Rautenberg, M., "Blade Excitation by Circumferentially Asymmetric Rotating Stall in Centrifugal Compressors," American Society of Mechanical Engineers, ASME Paper 92-GT-148, 1992.

[4]Day, I. J., "Stall Inception in Axial Flow Compressors," *Journal of Turbomachinery*, Vol. 115, No. 1, 1991, pp. 1–9.

[5]McDougall, N. M., Cumpsty, N. A., and Hynes, T. P., "Stall Inception in Axial Compressors" *Journal of Turbomachinery*, Vol. 112, No. 1, 1990, pp. 116–125.

[6]Garnier, V. H., Epstein, A. H., and Greitzer, E. M., "Rotating Waves as a Stall Inception Indication in Axial Compressors," *Journal of Turbomachinery*, Vol. 113, No. 2, 1990, pp. 299–302.

[7]Lawless, P. B., and Fleeter, S., "Rotating Stall Acoustic Signature in a Low Speed Centrifugal Compressor: Part 2—Vaned Diffuser," American Society of Mechanical Engineers, ASME Paper 93-GT-254, 1993.

[8]Day, I. J., and Freeman, C., "The Unstable Behavior of Low and High Speed Compressors," American Society of Mechanical Engineers, ASME Paper 93-GT-26, 1993.

[9]Wilson, A. G., and Freeman, C., "Stall Inception and Development in an Axial Flow Aeroengine," American Society of Mechanical Engineers, ASME Paper 93-GT-2, 1993.

[10]Ffowcs Williams, J. E., and Graham, W. R., "An Engine Demonstration of Active Surge Control," American Society of Mechanical Engineers, ASME Paper 90-GT-224, 1990.

[11]Ffowcs Williams, J. E., Harper, M. F. L., and Allwright, D. J., "Active Stabilization of Compressor Instability and Surge in a Working Engine," American Society of Mechanical Engineers, ASME Paper 92-GT-88, 1992.

[12]Oakes, W., Shook, P., McGuire, R., and Fleeter, S., "Aerodynamic Performance and Instability Initiation of a High Speed Research Centrifugal Compressor," *International Journal of Turbo and Jet Engines*, Vol. 14, No. 4, 1997, pp. 187–199.

[13]Frigne, P., and Van Den Braembussche, R., "Distinction Between Different Types of Impeller and Diffuser Rotating Stall in a Centrifugal Compressor With Vaneless Diffuser," *Journal of Engineering for Gas Turbines and Power*, Vol. 106, April 1984, pp. 468–474.

[14]Greitzer, E. M., "The Stability of Pumping Systems—The Freeman Scholar Lecture," *Journal of Fluids Engineering*, Vol. 103, June 1981, pp. 193–242.